

# Role of diffusion-weighted imaging for detecting bone marrow infiltration in skull in children with acute lymphoblastic leukemia

Weiguo Cao  
Changhong Liang  
Yungan Gen  
Chen Wang  
Cailei Zhao  
Longwei Sun

## PURPOSE

We aimed to determine whether diffusion-weighted imaging (DWI) with apparent diffusion coefficient (ADC) measurement can detect skull bone marrow infiltration in newly diagnosed acute lymphoblastic leukemia (ALL) children before therapy and normalization in complete remission after treatment.

## METHODS

Fifty-one newly diagnosed acute lymphoblastic leukemia (ALL) patients and 30 healthy age-matched subjects were included. Cranial magnetic resonance imaging (MRI) scans were reviewed, and skull marrow ADC values were compared before treatment and in complete remission after therapy.

## RESULTS

Skull marrow infiltration, manifested with abnormal DWI signals, was present in 37 patients (72.5%) before treatment. Of these, 23 (62.2%) showed scattered signal abnormalities and 14 (37.8%) showed a uniform abnormal signal pattern. Compared with the control group, ADC was significantly decreased in patients with ALL. DWI signal intensity and ADC normalized in patients with complete remission.

## CONCLUSION

DWI is a useful and noninvasive tool for detecting skull infiltration in ALL children before treatment and normalization at complete remission after therapy, and it is superior to conventional MRI in terms of conspicuity of these lesions. DWI could be used as an MRI biomarker for evaluation of treatment in ALL children.

Leukemia is the most common cancer in children, with acute lymphoblastic leukemia (ALL) being the most frequently diagnosed type (1), and its incidence is on the rise. The five-year event-free survival estimate in ALL children after treatment approaches 90% (2).

Although peripheral blood count, bone marrow aspiration, and biopsy provide the most important clues for diagnosis of acute leukemia in children, some acute leukemic patients may not have typical clinical manifestations and instead may present with abnormal magnetic resonance imaging (MRI) findings in the bone marrow (3, 4), especially when MRI is done before a clinical diagnosis of ALL. Thus, brain MRI can provide valuable information in skull bone marrow infiltration, which in some patients show pathologic changes earlier than peripheral blood count, bone marrow aspiration, and biopsy. Furthermore, some authors found that MRI findings may represent different pathologic features (5, 6). Malignant bone marrow lesions appear hyperintense, while benign bone marrow lesions appear hypointense or isointense on diffusion-weighted images (DWI). Also, benign lesions have higher apparent diffusion coefficient (ADC) than malignant lesions. These features can be used to distinguish leukemic patients from normal controls (7) and provide a helpful tool for accurate diagnosis and treatment monitoring (8), as well as predicting the prognosis and complete remission of leukemia (9). Thus, brain MRI is of value for both accurate diagnosis and patient management.

Brain MRI has often been used to assess for leukemia involvement of the central nervous system, mainly in ALL children with headache and vomiting. However, to our knowledge, there has been no published study concerning the use of DWI with ADC for examining ALL infiltration in the skull bone marrow. Furthermore, skull is thin and difficult to observe on DWI.

From the Department of Radiology (C.L. ✉ [cjr.lchh@vip.163.com](mailto:cjr.lchh@vip.163.com)), Guangdong Academy of Medical Sciences, Guangdong General Hospital, Guangzhou, China; Graduate College (W.C.), Southern Medical University, Guangdong General Hospital, Guangzhou, China; the Department of Radiology (W.C., Y.G., C.Z., L.S), Shenzhen Children's Hospital, Shenzhen, China; the Department of Neuroradiology (C.W.), Karolinska University Hospital, Stockholm, Sweden.

Received 6 May 2015; revision requested 22 July 2015; last revision received 29 March 2016; accepted 29 March 2016.

Published online 20 October 2016.  
DOI 10.5152/dir.2016.15167

In this study, we aimed to assess whether MRI, particularly DWI and ADC maps, is able to detect changes in skull marrow involvement before treatment and after complete remission in ALL patients.

## Methods

### Patients and control subjects

Fifty-one patients (29 boys and 22 girls, aged five months to 10 years; mean age, 3.7 years; median age, 3.3 years) admitted to our hospital between January 2011 and December 2012 were included in the study. They were clinically diagnosed as ALL and proven by bone marrow biopsy. All patients presenting with headache and vomiting had two brain MRI examinations, including DWI and ADC measurement, one before treatment and the second one after completion of treatments. The time interval of MRI examinations was 33–35 days. Patients who did not reach complete remission after 33 days of chemotherapy were not included.

A total of 30 age-matched control subjects (17 boys and 13 girls, aged seven months to 10 years; mean age, 4.3 years; median age, 4.6 years) studied with same MRI protocols were selected for comparison. Indications for MRI in these children were headache, convulsion, and dizziness. The exclusion criteria for control subjects were history of low birth weight or preterm delivery, musculoskeletal disorders, metabolic disorders, and systemic diseases. Children with history of treatment that might affect bone marrow were also excluded. They were proven to be healthy on follow-up visits.

Informed consent was obtained from the parents of all patients and control subjects

before entering this study, and the study was approved by the local ethics committee.

### Evaluation of brain parenchymal involvement and treatment response

Brain parenchymal involvement was defined as cerebrospinal fluid (CSF) examination including increased opening pressure ( $>200$  mm of  $H_2O$ ), increased white blood cell count ( $>0.01 \times 10^9/L$ ), elevated protein ( $>450$  mg/L), and presence of leukemic cells.

Complete remission was defined as normal cellular bone marrow containing fewer than 5% blast cells, normal peripheral neutrophil count ( $>1.5 \times 10^9/L$ ), and platelet count ( $>100 \times 10^9/L$ ) with no circulating blast cells.

### MRI examination

Brain MRI examinations were performed using a 1.5 T system (Signa, GE Medical Systems) with a quadrature head coil. All patients and control subjects underwent standard MRI with the following sequences: axial and sagittal T1-weighted fast spin-echo, axial T2-weighted fast spin-echo, and axial fluid-attenuated inversion recovery. Images were acquired with 24×24 cm field of view; 128×128 matrix size; 5 mm slice thickness with a 1.2 mm gap.

DWI was performed using spin-echo, echo-planar imaging with TR/TE 6000/106 ms, and b values of 0 and 1000  $mm^2/s$  in three orthogonal directions. Other imaging parameters were same as the other pulse sequences. DWI data were processed and apparent diffusion coefficient (ADC) maps were generated using the on console software (Functool 2, GE Medical System). ADC calculation was made by manually drawing 5–8  $mm^2$  regions of interest (ROI) in the skull marrow. Usually a total of six ROIs, which strictly corresponded to the locations of skull bone marrow on T1-weighted and T2-weighted images, were placed in frontal and occipital bones near the midline taking care to avoid cranial sutures, and parietal and greater wing of sphenoid bones bilaterally (Fig. 1). In ALL patients who had only local skull marrow involvements, the ROIs were placed in areas with abnormal signal intensities close to the standard sites. The ROIs were placed first on diffusion-weighted images, and then autocopied to ADC maps by console software. The mean ADC values were calculated by measuring frontal and occipital bones six times, and parietal and greater wing of sphenoid bones

six times; three times on the left and three times on the right side.

Two neuroradiologists (ten and nine years of experience in pediatric MRI, respectively) reviewed MRI findings and the ROIs carefully chosen on ADC maps. They were blinded to age, sex, and other pertinent clinical histories. Any discrepancies in image interpretation and ROI placement were resolved by consensus. ADC values were independently measured by two readers. Signal intensity of the skull marrow was assessed on conventional T1- and T2-weighted images and DWI. Abnormal signal intensity was judged as hypointense or hyperintense in relation to the adjacent muscle in the same section. On DWI, abnormal signal intensity was defined as hypointense or hyperintense to the adjacent fat in the same section when the little muscle was difficult to observe. The patterns of signal abnormality in the skull bone marrow infiltration were categorized into one of two groups as follows: “scattered group” showed multiple scattered locations of higher signal intensity in the low-signal-intensity marrow on diffusion-weighted images; “uniform group” showed uniformly high-signal-intensity marrow compared with the low-signal-intensity muscles on diffusion-weighted images. Abnormal signal intensity in brain parenchyma was compared with the adjacent normal gray matter; patients with abnormal signal intensity in brain parenchyma underwent lumbar puncture for CSF examination.

### Statistical analysis

Descriptive statistics of continuous variables are given as mean, standard deviation, and median. Paired t test was used to compare ADC values measured in ALL patients before start of treatment and after treatment at complete remission. Two independent samples t test was used to compare age and ADC values between patients and control subjects. Chi-square test was used to compare the difference between T1-weighted, T2-weighted, and diffusion-weighted images. To evaluate the bias of repeated ADC measurements, paired t test was used to compare ADC values between readers. The inter-reader agreement of ADC was evaluated with interclass correlation coefficients (ICC). ICC interclass correlation coefficient is interpreted as follows: 0.61–0.80, good agreement; 0.81–1.00, excellent agreement (10). The level of significance was set at  $P < 0.05$ .

#### Main points

- Diffusion-weighted imaging (DWI) signal intensity and apparent diffusion coefficient (ADC) values are useful to detect skull infiltration in acute lymphoblastic leukemia (ALL) children before treatment and normalization at complete remission (CR) after therapy.
- DWI can be helpful to identify the patterns of the skull involvement in ALL children.
- Skull marrow involvement was far more frequent than diffusion-weighted brain parenchymal involvement in ALL children. However, the skull marrow infiltration was frequently missed in this cohort.

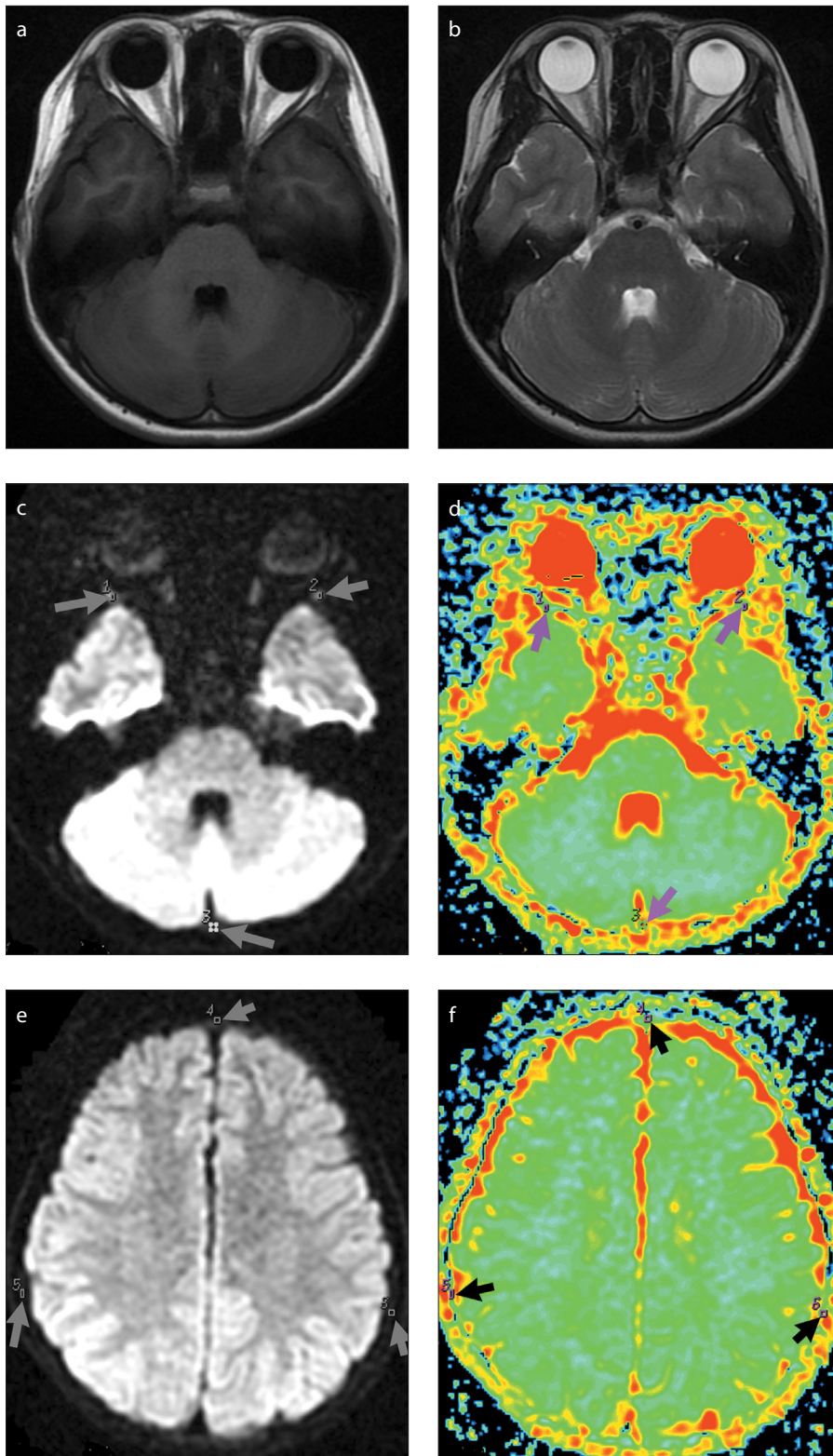


**Figure 1.** a–f. Magnetic resonance images of a 63-month-old male control subject. Axial T1-weighted image (a) shows slight hyperintensity of the skull marrow. Axial T2-weighted image (b) shows slight hypointensity of the skull marrow. Diffusion-weighted images (c, e) show slight hyperintensity of the skull marrow. ADC maps (d, f) show ADC measured in the regions of interest 1–6 (arrows).

## Results

Neuroradiologists reached an agreement in signal characteristics of all MRI

examinations of ALL patients and control subjects. Of 51 patients with ALL, four (7.8%) had brain parenchymal involve-

ment confirmed by CSF examination and 37 (72.5%) had abnormal signal changes in the skull bone marrow diagnosed as leukemia infiltration. Brain parenchymal involvement was present with multifocal hemorrhage and masses (Table 1). There were significant differences in the total number of abnormal signal of skull marrow involvement detected by DWI compared with T1-weighted ( $P = 0.001$ ) and T2-weighted ( $P = 0.003$ ) images. No significant difference in the total number of abnormal signal of skull marrow involvement was observed between T1- and T2-weighted images ( $P = 0.687$ ) (Table 1).

Two different patterns of signal abnormality were observed in the skull marrow, either unevenly scattered in different areas or uniform in almost all skull bones (Fig. 2). A total of 23 patients (62.2%) showed a scattered pattern of marrow infiltration and 14 patients (37.8%) exhibited a uniform pattern of infiltration. The characteristics and locations of abnormal signal intensities at the initial diagnosis are summarized in Table 1.

ADC values calculated by two readers are summarized in Table 2. There were no significant differences between readers in measuring ADC, with  $P$  values ranging from 0.752 to 0.993. Inter-reader agreements of ADC were good and excellent, with ICCs ranging from 0.79 to 0.99. Only the results for ADC measured by reader 1 were shown because of strong inter-reader agreement.

All pretreatment ALL patients with signs of bone marrow infiltration had significantly lower mean ADC than that of the control subjects. Further analyses showed that there was a significant difference in mean ADC between the control subjects and the pretreatment patients with hyperintensity diagnosed as marrow infiltration ( $P < 0.001$ ), but no significant difference compared with the pretreatment patients with normal signal intensity in the skull marrow, with  $P$  values ranging from 0.591 to 0.869 (Table 3). All patients with complete remission had normalized signal intensity in the skull marrow and normal mean ADC values compared with the control subjects (Table 3 and Fig. 3).

## Discussion

In our study, signal changes of the bone marrow infiltration were typically hypointense on T1-weighted images, and hyperintense on T2-weighted images and DWI. On DWI, skull marrow infiltration was detected in 37 patients (72.5%) before treatment. Mean ADC value was marked-

ly decreased in patients before treatment. Both DWI signal intensities and mean ADC values became normal in patients with complete remission. Brain MRI has been frequently used for evaluation of leukemia

infiltration in patients with ALL, and usually one or more DWI sequences are included in modern MRI protocols as they are less time consuming and more robust in lesion detection and differentiation. However, these

examinations are most often referred for intracranial pathologies and therefore lesions in the skull bone marrow, especially diffusely distributing lesions like leukemia infiltration, might be easily neglected. MRI is well suited for investigating bone marrows since signal intensities are directly related to the relative amount of fat, water, and cellular components in the marrow (11–13). The composition of bone marrow varies both with age and anatomic location. At birth and throughout early childhood, the marrow is predominantly hematopoietic and red in color. Hematopoietic marrow is thereafter gradually converted to fatty yellow marrow (14–16). On MRI this shows as a gradually increased signal on T1-weighted images accompanied by decreasing signal on T2-weighted and DWI images in the bone marrow. Conversely, with the bone marrow infiltration in ALL children, the tumor-related hypercellularity shows a decreased signal on T1-weighted images and an increased signal on T2-weighted and DWI images. Theoretically, there might be age-related diffusion signal changes in the bone marrow, but these changes are subtle on spin-echo images and give rise to few difficulties for differential diagnosis in children (17). Thus, in our study, using a spin-echo sequence for image acquisition, the age-related changes in skull bone marrow in DWI were minimal.

As a method based on the random movement of water molecules in tissues, DWI in combination with mean ADC measurements is sensitive to the change of propor-

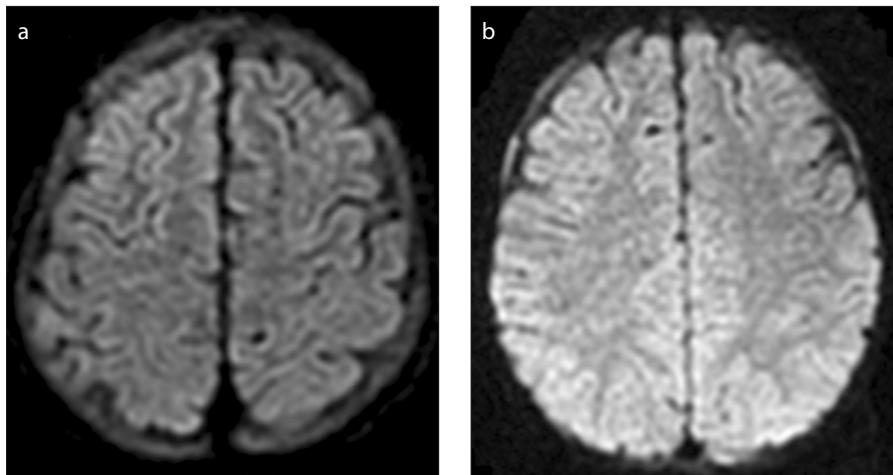


**Figure 2.** a, b. Diffusion-weighted images showing different patterns of signal abnormalities in the skull marrow of patients with acute leukemia before treatment. Image (a) shows a uniform pattern in a 23-month-old female patient. Image (b) shows a scattered pattern in a five-year-old male patient.

Table 1. Abnormal signal with initial MRI in children with acute lymphoblastic leukemia		
	Parenchymal involvement	Skull marrow
	n	n (%)
T1-weighted image	4	20 (39.2)
T2-weighted image	4	22 (43.2) <sup>a</sup>
Diffusion-weighted image	4	37 (72.5) <sup>b, c</sup>
Total number of patients	4*	51

<sup>a</sup>P = 0.687 (vs. T1-weighted image); <sup>b</sup>P = 0.001 (vs. T1-weighted image); <sup>c</sup>P = 0.003 (vs. T2-weighted image).  
\*There were three patients with both brain parenchymal and skull involvement and one patient with only parenchymal involvement.

Table 2. ADC of six structures from skull marrow measured by two readers ( $\times 10^{-3}$ mm <sup>2</sup> /s)							
		Frontal bone	Greater wing of sphenoid bone		Occipital bone	Parietal bone	
			Right	Left		Right	Left
Control subjects (n=30)	Reader1	1.30±0.42	1.58±0.43	1.42±0.37	1.50±0.63	1.97±0.50	1.87±0.58
	Reader2	1.29±0.44	1.61±0.39	1.39±0.42	1.49±0.59	1.96±0.48	1.89±0.57
ALL patients (n=51)	Reader1	0.86±0.55	0.95±0.54	0.91±0.46	0.96±0.52	1.14±0.68	1.07±0.67
	Reader2	0.84±0.52	0.96±0.52	0.93±0.47	0.96±0.49	1.09±0.63	1.11±0.65
Hyperintensity (n=37)	Reader1	0.69±0.44	0.77±0.39	0.79±0.41	0.82±0.38	0.91±0.50	0.87±0.48
	Reader2	0.68±0.42	0.78±0.41	0.81±0.43	0.85±0.43	0.96±0.54	0.92±0.46
Normal intensity (n=14)	Reader1	1.32±0.44	1.56±0.49	1.42±0.37	1.51±0.64	2.02±0.38	1.83±0.51
	Reader2	1.30±0.46	1.60±0.51	1.45±0.39	1.53±0.67	1.96±0.66	1.86±0.56
Complete remission (n=51)	Reader1	1.28±0.52	1.60±0.38	1.41±0.47	1.53±0.51	1.98±0.42	1.91±0.47
	Reader2	1.28±0.56	1.63±0.44	1.46±0.52	1.56±0.57	2.03±0.57	1.98±0.43

Data are presented as mean±standard deviation. ADC, apparent diffusion coefficient.

**Table 3.** ADC of six structures from skull marrow in pretreatment patients, complete remission patients, and healthy control subjects ( $\times 10^{-3}$  mm<sup>2</sup>/s)

	Frontal bone	Greater wing of sphenoid bone		Occipital bone	Parietal bone	
		Right	Left		Right	Left
Control subjects (n=30)	1.30±0.42	1.58±0.43	1.42±0.37	1.50±0.63	1.97±0.50	1.87±0.58
ALL patients (n=51)	0.86±0.55	0.95±0.54	0.91±0.46	0.96±0.52	1.14±0.68	1.07±0.67
Hyperintensity (n=37)	0.69±0.44	0.77±0.39	0.79±0.41	0.82±0.38	0.91±0.50	0.87±0.48
Normal intensity (n=14)	1.32±0.44	1.56±0.49	1.42±0.37	1.51±0.64	2.02±0.38	1.83±0.51
Complete remission (n=51)	1.28±0.52	1.60±0.38	1.41±0.47	1.53±0.51	1.98±0.42	1.91±0.47
<i>P</i> control vs. ALL patients	0.002	<0.001	<0.001	0.001	<0.001	<0.001
<i>P</i> control vs. hyperintensity	<0.001	<0.001	<0.001	<0.001	<0.001	<0.001
<i>P</i> control vs. normal intensity	0.651	0.632	0.869	0.695	0.626	0.591
<i>P</i> ALL patients vs. complete remission	0.003	<0.001	0.001	<0.001	<0.001	<0.001
<i>P</i> hyperintensity vs. normal intensity	<0.001	<0.001	<0.001	<0.001	<0.001	<0.001
<i>P</i> hyperintensity vs. complete remission	0.001	<0.001	<0.001	<0.001	<0.001	<0.001

Data are presented as mean±standard deviation.  
ADC, apparent diffusion coefficient.

tions in tissue components, particularly in cellular densities. This technique was proven useful in the assessment of bone marrow pathologies and metastatic marrow diseases (18, 19). Some studies utilized conventional MRI to evaluate signal characteristics of cranial marrow (14, 18, 20–22). Some authors found that MRI findings could be used as predictors for distinguishing leukemic patients from normal controls, providing more accurate diagnosis (7). To the best of our knowledge, no report on the evaluation of skull marrow infiltration in pediatric ALL patients using DWI and mean ADC measurements was published before. This study aimed to research ALL infiltration in a new osseous area in the skull by conventional brain MRI, which is frequently performed on these patients in our institution since it is simpler than whole-MRI.

We found skull marrow involvement in 72.5% of our ALL patients, which is far more frequent than the percentage of brain parenchymal involvement (7.8%) in our patient group. The skull marrow infiltration was frequently missed in our initial clinical reports, mainly because attentions were often directed to scrutinize parenchymal malignancies such as granulocytic sarcoma, which may rarely occur with lymphocytic leukemia (23, 24), and diffuse involvement in the skull marrow did not show striking signal changes on conventional T1- and T2-weighted images.

In the retrospective analysis of our series, 39.2% of ALL children showed signal abnormalities on T1-weighted images and

43.2% showed signal abnormalities on T2-weighted images. However, 72.5% of patients showed pronounced signal changes on DWI images. On these images, the skull marrow infiltration in ALL patients were visualized with a markedly hyperintense signal and correspondingly reduced mean ADC value, which is indicative of restricted water diffusion. The mean ADC value in our patients with skull marrow infiltration was  $0.81 \pm 0.43 \times 10^{-3}$  mm<sup>2</sup>/s, which is similar to the mean ADC value for cranial metastases, previously reported as  $0.90 \pm 0.25 \times 10^{-3}$  mm<sup>2</sup>/s (25, 26). One of the factors that may influence the ADC measurement is the b value setup. In a given magnetic field a higher b value will result in a lower ADC. Another factor is variation in MRI scanners; a phantom study has shown that ADC values varied significantly across different MRI systems (27). Furthermore, the surrounding structure may also influence the ADC measurements, which is why multiple measurements were performed in our study to increase the accuracy.

Several factors may contribute to diffusion restriction. Probably, the main reason is the hypercellularity of leukemic tissues, which is generated by bone marrow hyperplasia, the main pathologic feature of skull marrow infiltration in ALL (25, 26). Furthermore, diffusion restriction is enhanced by the limited transmembranous microscopic movement due to the decreased amount of intracellular water. An early study has shown that the signal intensity ratio of the bone marrow infiltration may reflect tumor

burden; the lower the intensity, the higher the ratio of leukemic cells (28). When skull marrow involvement in ALL children was treated successfully to the state of complete remission, tumor cell death resulted in increased water diffusivity manifested as decreased signal intensity on DWI and increased ADC values (29).

The signal changes on DWI are not specific, and therefore could not be used solely to distinguish ALL marrow involvement from other marrow infiltrative pathologies such as other hematologic diseases, metastases, and multiple myeloma. Thus, DWI findings cannot definitively diagnose ALL. The diagnosis of ALL marrow infiltration should be closely correlated with other clinical findings and laboratory analyses, including bone marrow biopsy.

Although bone marrow biopsy is useful and necessary in the diagnosis and assessment of treatment response in ALL children, it is an invasive examination. Our study demonstrated that DWI is a noninvasive and very sensitive tool for observing changes of skull bone marrow in ALL patients. It is easy to evaluate the treatment response by changes in the skull marrow DWI findings, and DWI is helpful to reduce the number of bone marrow biopsies and better select children that must undergo this examination.

One limitation of the study in using DWI for observation of skull bone marrow was the intrinsic physical properties of the sequence, making it sensitive to artifacts and image distortions. Use of multi-shot echo-planar imaging and spin-echo based

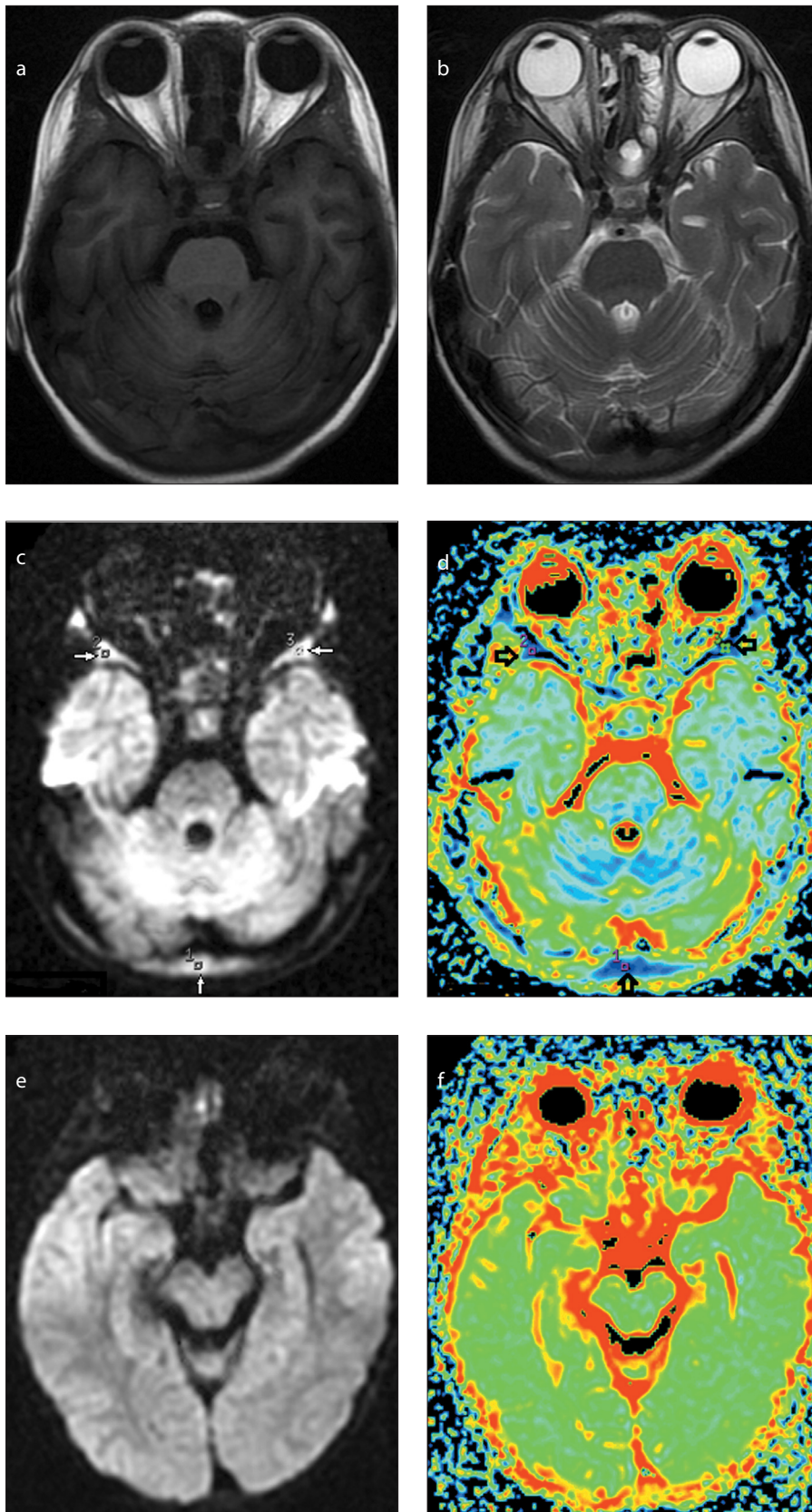


**Figure 3.** a–f. Magnetic resonance image of a two-year-old male patient with acute leukemia. Axial T1-weighted (a) and T2-weighted (b) images before treatment show isointensity of skull marrow, but on diffusion-weighted image (c) the marrow shows significant hyperintensity. ADC map (d) shows low ADC values in the regions of interest 1–3 (arrows). After treatment with clinical complete remission, diffusion-weighted image (e) shows markedly decreased signal intensity in the skull marrow, and ADC map (f) shows increased ADC correspondingly.

diffusion technique may help to minimize these technical problems. Another drawback was that the program supplied by the manufacture for data analyses could only produce color ADC maps, which was difficult to associate directly to signal intensity variations in gray-scale. An additional limitation of our study was the absence of pathologic correlation between ADC values and histology. Skull is thin and is usually not biopsied in acute leukemic children.

In conclusion, skull marrow infiltration in children with initial ALL was visualized as a markedly hyperintense signal on DWI, which is a more advantageous sequence for detecting skull infiltrations than T1- and T2-weighted imaging. The decrease in the mean ADC value indicated diffusion restriction due to hypercellularity of tumor tissues. When complete clinical remission was achieved following successful treatment, DWI signal abnormalities, as well as mean ADC values, recuperated. Our study describes the MRI characteristics of skull bone marrow infiltration in children with ALL and suggests DWI as a tool for treatment monitoring.

#### Acknowledgements

The authors wish to thank the patients and their families for participating in the study. This research received no specific grant from any funding agency in the public, commercial, or not-for-profit sectors.

#### Conflict of interest disclosure

The authors declared no conflicts of interest.

#### References

1. Smith MA, Gloeckler Ries LA, Gurney JG, Ross JA. Leukemia SEER pediatric monograph. In: Gloeckler Ries LA, Smith MA, Gurney JG, et al, eds. Cancer incidence among children and adolescents: United States SEER program 1975–1995. Bethesda: National Cancer Institute, 1999; 17–34.
2. Pui CH, Evans WE. Treatment of acute lymphoblastic leukemia. *N Engl J Med* 2006; 354:166–178. [\[CrossRef\]](#)
3. Kato M1, Koh K, Kikuchi A, et al. Case series of pediatric acute leukemia without a peripheral blood abnormality, detected by magnetic resonance imaging. *Int J Hematol* 2011; 93:787–790. [\[CrossRef\]](#)
4. Lu CS, Huang IA, Wang CJ, Lo WC, Jaing TH. Magnetic resonance abnormalities of bone marrow in a case of acute lymphoblastic leukemia. *Acta Paediatr Taiwan* 2003; 44:109–111.
5. Nonomura Y, Yasumoto M, Yoshimura R, et al. Relationship between bone marrow cellularity and apparent diffusion coefficient. *J Magn Reson Imaging* 2001; 13:757–760. [\[CrossRef\]](#)
6. Dietrich O, Biffar A, Reiser MF, Baur-Melnyk A. Diffusion-weighted imaging of bone marrow. *Semin Musculoskelet Radiol* 2009; 13:134–144. [\[CrossRef\]](#)
7. Nishiji T, Kono AK, Akasaka Y, et al. Bone marrow magnetic resonance imaging of the clavus in pediatric leukemia patients and normal controls. *Jpn J Radiol* 2015; 33:146–152. [\[CrossRef\]](#)

8. Daldrup-Link HE, Henning T, Link TM. MR imaging of therapy-induced changes of bone marrow. *Eur Radiol* 2007; 17:743–761. [\[CrossRef\]](#)
9. Wang J, Zhang X, Niu J. Clinical significance of magnetic resonance imaging of bone marrow in patients with leukemia. *J Tongji Med Univ* 2001; 21:242–245. [\[CrossRef\]](#)
10. Curvo-Semedo L, Lambregts DM, Maas M, et al. Rectal cancer: assessment of complete response to preoperative combined radiation therapy with chemotherapy—conventional MR volumetry versus diffusion-weighted MR imaging. *Radiology* 2011; 260:734–743. [\[CrossRef\]](#)
11. Vogler JB, 3rd, Murphy WA. Bone marrow imaging. *Radiology* 1988; 168:679–693. [\[CrossRef\]](#)
12. Vande Berg BC, Malghem J, Lecouvet FE, Maldague B. Magnetic resonance imaging of normal bone marrow. *Eur Radiol* 1998; 8:1327–1334. [\[CrossRef\]](#)
13. Vande Berg BC, Malghem J, Lecouvet FE, Maldague B. Normal bone marrow: dynamic aspects in magnetic resonance imaging. *J Radiol* 2001; 82:127–135.
14. Ricci C, Cova M, Kang YS, et al. Normal age-related patterns of cellular and fatty bone marrow distribution in the axial skeleton: MR imaging study. *Radiology* 1990; 177:83–88. [\[CrossRef\]](#)
15. Kricun ME. Red-yellow marrow conversion: its effect on the location of some solitary bone lesions. *Skeletal Radiol* 1985; 14:10–19. [\[CrossRef\]](#)
16. Bracken J, Nandurkar D, Radhakrishnan K, Ditchfield M. Normal paediatric bone marrow: magnetic resonance imaging appearances from birth to 5 years. *J Med Imaging Radiat Oncol* 2013; 57:283–291. [\[CrossRef\]](#)
17. Daldrup-Link HE, Franzius C, Link TM, et al. Whole-body MR imaging for detection of bone metastases in children and young adults: comparison with skeletal scintigraphy and FDG PET. *AJR Am J Roentgenol* 2001; 177:229–236. [\[CrossRef\]](#)
18. Moon WJ, Lee MH, Chung EC. Diffusion-weighted imaging with sensitivity encoding (SENSE) for detecting cranial bone marrow metastases: comparison with T1-weighted images. *Korean J Radiol* 2007; 8:185–191. [\[CrossRef\]](#)
19. Padhani AR, van Ree K, Collins DJ, D'Sa S, Makris A. Assessing the relation between bone marrow signal intensity and apparent diffusion coefficient in diffusion-weighted MRI. *AJR Am J Roentgenol* 2013; 200:163–170. [\[CrossRef\]](#)
20. Kimura F, Kim KS, Friedman H, Russell EJ, Breit R. MR imaging of the normal and abnormal clivus. *AJR Am J Roentgenol* 1990; 155:1285–1291. [\[CrossRef\]](#)
21. Okada Y, Aoki S, Barkovich AJ, et al. Cranial bone marrow in children: assessment of normal development with MR imaging. *Radiology* 1989; 171:161–164. [\[CrossRef\]](#)
22. Eustace S, McGrath D, Albrecht M, Fogt F, Buff B, Longmaid HE. Clival marrow changes in AIDS: findings at MR imaging. *Radiology* 1994; 193:623–627. [\[CrossRef\]](#)
23. Ahn JY, Kwon SO, Shin MS, Kang SH, Kim YR. Meningeal chloroma (granulocytic sarcoma) in acute lymphoblastic leukemia mimicking a falx meningioma. *J Neurooncol* 2002; 60:31–35. [\[CrossRef\]](#)
24. Lee SH, Park J, Hwang SK. Isolated recurrence of intracerebral granulocytic sarcoma in acute lymphoblastic leukemia: a case report. *J Neurooncol* 2006; 80:101–104. [\[CrossRef\]](#)
25. Shen J, Liang B. MR imaging of bone marrow in common hematological disease. *Chinese Comput Med Imaging* 2003; 9:338–348.
26. Herneth AM, Friedrich K, Weidekamm C, et al. Diffusion-weighted imaging of bone marrow pathologies. *Eur J Radiol* 2005; 55:74–83. [\[CrossRef\]](#)
27. Kolff-Gart AS, Pouwels PJW, Noij DP, et al. Diffusion-weighted imaging of the head and neck in healthy subjects: reproducibility of ADC values in different MRI systems and repeat sessions. *AJNR Am J Neuroradiol* 2015; 36:384–390. [\[CrossRef\]](#)
28. Shen J, Liang B. Quantitative MR imaging of bone marrow in leukemia. *Aizheng* 2003; 22:291–294.
29. Ballon D, Dyke J, Schwartz LH, et al. Bone marrow segmentation in leukemia using diffusion and T2-weighted echo planar magnetic resonance imaging. *NMR Biomedicine* 2000; 13:321–328. [\[CrossRef\]](#)